J Mol Model (2008) 14:705–716
DOI 10.1007/s00894-008-0285-0

ORIGINAL PAPER

Comparison of the electronic properties, and thermodynamic and kinetic parameters of the aquation of selected platinum (II) derivatives with their anticancer IC_{50} indexes

Ondřej Bradáč · Tomáš Zimmermann · Jaroslav V. Burda

Received: 20 November 2007 / Accepted: 6 February 2008 / Published online: 6 March 2008

Abstract Three potential anticancer agents {trans-[$PtCl_2$ (NH_3)(thiazole)], cis-[$PtCl_2$(NH_3)(piperidine)], and $PtCl_2$ (NH_3)(cyclohexylamine) (JM118)} were explored and compared with cisplatin and the inactive $[PtCl(dien)]^+$ complex. Basic electronic properties, bonding and stabilization energies were determined, and thermodynamic and kinetic parameters for the aquation reaction were estimated at the B3LYP/6-311++G(2df,2pd) level of theory. Since the aquation process represents activation of these agents, the obtained rate constants were compared with the experimental IC_{50} values for several tumor cells. Despite the fact that the processes in which these drugs are involved and the way in which they affect cells are very complex, some correlations can be deduced.

Keywords Platinum drugs · Density functional theory calculations · Thermodynamics · Rate constants

Introduction

Since Rosenberg's discovery of the anticancer activities of cisplatin [1], platinum complexes present one of the most important group of anticancer metallodrugs. Many platinum compounds [both Pt(II) and Pt(IV)] have been investigated in the search for new, more efficient drugs with better properties (fewer side-effects, lower toxicity). These medical studies are supported by many in vivo and in vitro experiments—an immense pool of studies from which a few representatives [2–14] can be mentioned. Another reason to find more suitable derivatives of platinum complexes (as well as other transition metals) is the resistance of tumor cells to cisplatin, whether acquired (when administered repeatedly) or intrinsic. In this context, second- and third-generations of such drugs ([e.g., carboplatin, oxaliplatin, Pt(IV) complex JM216, ADM473 or trinuclear BBR 3464] have been discovered. Recently, cisplatin and carboplatin have joined the group of "most often administrated" drugs [15]. They have the same final DNA adduct (also common to some other platinum drugs): a cis-$[Pt(NH_3)_2$-1,2-d(GpG)$]^{2+}$ fragment. Such adducts cause a roll of 25–50 degrees between the guanine bases involved in the cross-link, and a global bend of the helix axis towards the major groove of about 20–40 degrees [16–20]. The molecular structure of these complexes was determined at high resolution (2.6 Å) by Dickerson's group [21]. An analogous structure containing the cisplatin G-Pt-G bridge [16] was solved at similar resolution. The distortion of DNA caused by cisplatin was described by Lilley [22]. Cisplatin can also form interstrand bridges [23]. The cross-linked adduct of oxaliplatin with 1,2-d(GpG) intrastrand bases of a DNA oligomer was studied by Spingler et al. [24]. Lately, other adducts of platinum complexes with DNA [25, 26] as well as the ternary complex of the DNA oligomer with cisplatin and HMG-proteins [27, 28] were crystallized and described. Quaternary platinum complexes in solution were explored by Sigel and Lippert [29]. Various conformers of the cisplatin adduct with d(GpG), the structures of phosphodiester backbone was also discussed, were examined by Marzilli and coworkers [30], who combined NMR and CD spectroscopy with computational simulations. Recently, a study on cisplatin derivatives was published by Reedijk et al. [31].

O. Bradáč · T. Zimmermann · J. V. Burda (✉)
Department of Chemical Physics and Optics,
Faculty of Mathematics and Physics, Charles University,
Ke Karlovu 3,
121 16 Prague 2, Czech Republic
e-mail: burda@karlov.mff.cuni.cz

Recently, platinum(IV) complexes have also been extensively explored [32–36]. These compounds have relatively high stability, which enables oral administration. In their subsequent pathway, they are metabolized and reduced to four-coordinated platinum(II) analogues [37, 38].

Detailed insight into molecular (physico-chemical) descriptions can also be achieved by computational modeling, which reveals the structural and bonding relationships in the formation of platinum complexes with DNA bases, amino acid side chains and other systems. Many computational studies of Pt-nucleobases interactions have been published. The possibility of using CPMD (Carr-Parinello molecular dynamics) and hybrid molecular mechanics/CPMD techniques for the calculation of structural and spectroscopic information on novel platinum-based anticancer drugs is discussed by Dal Peraro et al. [39]. The effect of N7 platination on the strength of the N9-C1′ glycosyl bond of purine bases was revealed in a study by Baik et al. [40]. The reaction mechanism of the formation of $Pt(NH_3)_2$diguanine complexes was also investigated [41]. A similar study was published by Raber et al. [42], where both reaction steps creating the mononucleobase and dinucleobase complexes were considered. The first step, formation of a single-base adduct, was also explored by Chval and Šíp [43]. Dos Santos et al. [44] studied the structure and properties of an anhydrotetracycline-Pt(II) complex together with the aquation reaction. They found the rate constant to be similar to that of the cisplatin complex. Another two papers from this laboratory deal with the description of cisplatin in (explicitly treated) a water solution using the Monte Carlo simulation [45], or interaction of cisplatin with guanine [46]. Our group has studied the thermodynamics of Pt-bridges, bonding energy parameters, and the influence of a sugar-phosphate backbone [47–50]. The calculation of a Pt-thiazole complex was performed by Chang et al. [51]. Recently, a study of the influence of GC base-pairing on Pt complexes was published [52], which discusses the possibility of interbase proton transfer from G to C. Robertazzi and Platts have carried out QM/MM calculations of the cisplatin adduct with an octamer of double-stranded DNA sequence [53]. Wysokinski et al. investigated characterization of the structural and vibrational spectra of an (orotato)platinum (II) complex [54]. These latter authors compared the calculated (DFT/mPW1PW91) values of vibration transitions with experimental data. Some novel trans-platinum(II) anticancer drugs (with aliphatic amines) have been studied at the B3LYP level [55], and aquation processes were also examined. DFT techniques with the VTZP basis set were used by Deubel [56] to compare the affinities of cisplatin to S-sites and N-sites of amino acids and DNA bases. Deubel's results are in very good agreement with our previous calculations of the thermodynamics of aquation of platinum complexes [57–60], and the interactions with sulfur-containing amino acids [61, T. Zimmermann and J.V. Burda, manuscript submitted]. Recently, dinuclear [62] and trinuclear [63] (BBR3464) platinum(II) complexes have also been studied using a computational approach. An aquation study of carboplatin was performed by Pavelka et al. [64], in which a relatively high activation barrier of 30 kcal mol^{-1} was suggested based on the B3LYP/6-31++G (2df,2pd) computational level. A discussion of the correlation between thermodynamic and kinetic data and theoretical calculations of Pt(II) complexes was published by Hofmann et al. [65]. Ziegler and co-workers have published several studies on the behavior and properties of platinum complexes, e.g. [66]. In one of these studies, the activation of methane by $[PtCl_4]^{2-}$ in acidic aqueous solution was examined. The authors have shown that a complex with two water molecules is the most active in the H/D exchange reaction [67]. Some aspects of cisplatin hydrolysis are discussed by Tsipis and Sigalas [68]. For other studies on aquation of Pt(II) complexes, see [69–75].

Based on the above-mentioned experimental and computational results, the aim of this study is to explore selected platinum(II) derivatives. It should be pointed out that each of the three selected complexes is a derivative of cisplatin or transplatin isomer where one NH_3 is replaced by another nitrogen-containing ligand, either thiazole, piperidine or cyclohexylamine. Since the electronic properties of compounds with anticancer activity have already been established, our computational results for the selected Pt(II) complexes will be compared with the 'certified' drug - cisplatin on the one hand, and an inactive species—the $[Pt(dien)Cl]^-$ complex—on the other. The activation process of Pt-complexes is an important step and therefore we decided to compare the thermodynamic and kinetic parameters of this activation process (aquation) with activity indexes (the IC_{50} for several different types of the cancer cells will be used).

Methods

Computational details

The set of compared compounds consists of $[PtCl(dien)]^+$ (chlorodiethylenetriamine-platinum(II) chloride, Pt-Dien) (a complex with very low cytotoxic activity), trans-$[PtCl_2(NH_3)(thiazole)]$ (Pt-Tz) (reported recently [2] as a promising substance), cis-$[PtCl_2(NH_3)(piperidine)]$ (Pt-Pip) (a newly tested antitumor drug), $PtCl_2(NH_3)$(cyclohexylamine) (JM118—a metabolite of satraplatin JM216) and cisplatin (DDP) as a "benchmark". All the optimized geometries were obtained at the density functional theory

(DFT) level of theory with the B3LYP functional and the 6-31++G(d,p) basis set. Platinum, chlorine and sulfur atoms were described by the quasi-relativistic Stuttgart-Dresden energy-averaged effective core potentials {MWB-60 (Pt) [76] or MWB-10 (S and Cl) [77]}. The original pseudo-orbitals were augmented by a set of the appropriate diffuse and polarization functions [α_f(Pt)=0.998, α_d(Cl)=0.618, α_d(S)=0.499)] as shown in our previous studies, e.g. [57]. The same level was also used for frequency analyses. The single-point energies of the optimized structures, and stationary points from the aquation reaction profile were determined with the augmented triple-zeta basis set 6-311++G(2df,2pd), with a consistent extension of the Pt, S, and Cl pseudoorbitals. The ΔE^{Stab} stabilization energies were determined within the BSSE scheme according to the formula:

$$\Delta E^{Stab} = -\left(E_{complex} - \sum E_{ligand} - E_{Pt}\right) - \sum E^{deform}. \quad (1)$$

The deformation energies of all ligands were treated as the energy difference between the frozen ligand structure within complex geometry and the geometry of the optimized isolated ligand. The bonding and association energies were estimated from the following equation:

$$BE = E_{complex} - E_L - E_{CL}, \quad (2)$$

where E_L is the BSSE-corrected energy of the given ligand calculated with the ghost AO function on the complementary part of the whole complex, and E_{CL} its complement treated likewise.

Aquation, where the chloro ligand is replaced by a water molecule, was studied using a supermolecular approach with both interacting molecules considered as a single H-bonded system. The character of the transition states was confirmed by frequency analysis, in which a single negative eigenvalue of the hessian matrix corresponds to the appropriate antisymmetric stretching mode. In some cases, the global minimum of the reactant supermolecule does not correspond to the initial state of the reaction coordinate. Therefore, an additional local minimum has to be evaluated for such reaction course in order to obtain the correct potential energy surface (PES) for the determination of rate constant [60]. These constant were estimated from Eyring's theory of transition states (TST) according to formula:

$$k^{TST}(T) = \frac{kT}{h} \cdot \frac{F^{TS}}{F^{Pt}F^{w}} \cdot \exp\left(E_0/kT\right)$$

where F^X are the molecular partition functions per unit volume for TS, Pt-complex (isolated reactant molecule), and water, and E_0 is the energy of the activation barrier. The rate constants were evaluated by the program DOIT obtained from Smerdachina et al. [78]. The electronic structure calculations were performed using the Gaussian98 program package, and program NBO v. 5.0 (Wisconsin University [79]) was employed for evaluation of the natural bond orbital (NBO) characteristics.

Results and discussion

Four derivatives of cisplatin were first optimized as isolated complexes. Several electronic properties were evaluated and compared with the original drug. The aquation reactions of these platinum complexes was then explored.

Isolated complexes

All the chosen structures were optimized and the coordination bond lengths obtained are summarized in Table 1. It follows that the largest Pt–Cl distance occurs in the thiazole (Tz) complex (≈2.36 Å). This is clearly caused by the trans-influence effect since the chloro ligands are mutually in the trans positions. The propeller twist of the platinum plane and the plane of the thiazole ring is about 24°. In all remaining 2+ charged complexes, the Pt–Cl distances are about 2.33 Å. The shortest Pt–Cl bond is found in the

Table 1 The platinum–ligand (Pt–L) coordination distances (in Å) and density functional theory (DFT) dipole moments, μ (in D). *Pt-Dien* PtCl(dien)$^+$ [chlorodiethylenetriamine-platinum(II)], *Pt-Tz* trans-[$PtCl_2(NH_3)$(thiazole)], *Pt-Pip* cis-[$PtCl_2(NH_3)$(piperidine)], *JM118* $PtCl_2(NH_3)$(cyclohexylamine), *DDP* cisplatin

Complex	Pt-Cl_1[a]	Pt-Cl_2	Pt-N_{NH3}	Pt-N_X	μ
Pt-Dien	2.310	-	2.070[b]	2.072[c]	-
Pt-Tz	2.362	2.360	2.061	2.043	1.2
Pt-Pip	2.340	2.333	2.104	2.109	11.4
JM118	2.336	2.330	2.105	2.107	10.7
DDP	2.327	2.327	2.106	2.106	10.7

[a] Cl_1 is in trans position to X-ligand
[b] In cis-position to Cl atom of Pt-dien complex
[c] In trans-position to Cl atom of Pt-dien complex

$Pt[Cl(dien)]^+$ complex due to the weak competition of the three amino ligands. Consistent with the trend of Pt–Cl bonds, the shortest Pt–N bond also occurs in the complex containing the Tz ligand. Besides a weak trans-influence, a stronger donation from the Tz ligand than from ammonia was revealed. This effect is due to a π-back-donation, which was confirmed in the NBO analysis of this system. A perturbation energy within the NBO program of about 30 kcal mol^{-1} was obtained for donation from the Pt lone pair to the N (Tz) vacant orbital. Tz is the only ligand from this set of complexes to allow back-donation. The remaining Pt–N bond lengths are fairly similar (about 2.106 Å). Calculation of a hindered rotation of the thiazole ring around Pt–N(Tz) was also conducted. A very small rotational barrier (about 0.4 kcal mol^{-1}) was found, which means that thiazole can practically freely rotate. In the case of piperidine, this barrier is substantially higher (about 6 kcal mol^{-1}), demonstrating some sterical hindrance from the neighboring amino group.

The bonding and stabilization energies determined for all these structures are presented in Table 2. The most stable structure is the Pt-Tz complex because of the π-back-donation ability of Tz. Furthermore, very similar values for the remaining electroneutral complexes were revealed, which were in the following order: JM118 ≥ Pt-Pip >DDP. The same order also applies to the Pt–L bonding energy for the key ligand, and inversely to the Pt–Cl bond.

Table 1 lists the values of the dipole moments of the electroneutral complexes. The dipole moments of the explored cis-complexes have very similar values (μ≈11 D), due mainly to the arrangement of metal and chloro ligands. This explains the relatively small dipole moment of the trans-Tz complex since the Cl-Pt-Cl atoms are arranged almost linearly (forming an angle of 174°). In Table 3, partial charges from the natural population analysis (NPA) are displayed for both MP2 and B3LYP electron densities. Both computational levels provide a very similar qualitative picture of the electron distribution in the examined complexes. Positive values of the Pt charge indicate the extent of the donation from the various ligands. Relatively weaker donation occurs in the Pt-Dien complex because only one Cl ligand is present. In this complex, much less dative competition was found than in the remaining complexes. This is caused by the presence of only one dative bond with the negatively charged ligand (strongly electrostatically enhanced). Another system with a larger partial charge is the Pt-Tz complex, where the higher value is connected with the ability of the Tz ligand to accept back-donation from occupied Pt "π" d-AOs.

Aquation process

The replacement of a chloro ligand by water introduces an activation reaction when the Pt-complex reacts to the lower concentration of chloride anions in a cell, especially in the cell nucleus. Therefore, according to the Guldberg-Waage equilibrium law, formation of less stable aqua complexes are enforced. By analogy with our previous aquation studies on cisplatin [59, 60], a two-step reaction mechanism was adopted for the activation process. First, the less stable chloro ligand (according to already evaluated BE energies) is replaced by a water molecule. In order to keep the whole supermolecule electroneutral, the hydroxyl group is considered in the second step instead of the aqua ligand and the remaining chlorine is replaced by water.

Chlorodiethylenetriamine-platinum(II)

In the case of the diethylenetriamine complex $[PtCl(dien)]^+$, only the first aquation reaction is possible. The optimized supermolecular structures of reactants, transition state (TS) and products are displayed in Fig. 1. The most stable arrangement of the associated water molecule is, in this case, between the chloro- and one of the cis-amino-group. The coordination bonds are listed in Table 4. Some deformations of the platinum complex due to the associated water (in comparison with the bond lengths of the isolated complexes from Table 1) can be noted for the reactant state. The trend of elongation or shortening of the coordinated bonds along the reaction coordinates is the same as found in our previous study [59]. The activation barrier was found to be about 32 kcal mol^{-1}. This is the highest energy of all the explored set of complexes. The heat of aquation also shows the most endothermic process, as can be seen in Table 5, which summarizes the energetics of the aquation process.

Table 2 Bonding (BE), stabilization (Stab) and deformation (Deform) energies of the isolated complexes (in kcal mol^{-1})

Complex	BE(Pt-Cl_1)	BE(Pt-Cl_2)	BE(Pt-NH_3)	BE(Pt-X)	ΔE^{Stab}	ΔE^{Deform}
Pt-Dien	−243.0	-	-	−227.6	642.8	15.6
Pt-Tz	−155.7	−155.5	−54.2	−51.5	752.0	1.3
Pt-Pip	−148.5	−150.3	−38.3	−42.6	741.5	1.8
JM118	−151.0	−153.9	−38.9	−43.1	743.6	1.1
DDP	−160.7	−160.7	−39.8	−39.8	741.2	0.3

Table 3 The natural population analysis (NPA) partial charges for the key coordinating atoms (in e)

Complex	Method	Pt	Cl_1	Cl_2	$N_{NH3(cisI)}$	$N_{x(cisII)}$	N_{trans}
Pt-Dien	MP2	0.53	−0.45	-	−0.75	−0.75	−0.63
	DFT	0.59	−0.48	-	−0.76	−0.76	−0.64
Pt-Tz	MP2	0.52	−0.54	−0.54	−0.90	−0.44	-
	DFT	0.58	−0.56	−0.56	−0.91	−0.48	-
Pt-Pip	MP2	0.47	−0.49	−0.48	−0.95	−0.64	-
	DFT	0.53	−0.51	−0.51	−0.96	−0.65	-
JM118	MP2	0.47	−0.49	−0.48	−0.95	−0.76	-
	DFT	0.53	−0.49	−0.49	−0.95	−0.77	-
DDP	MP2	0.46	−0.48	−0.48	−0.96	−0.96	-
	DFT	0.52	−0.50	−0.50	−0.96	−0.96	-

Trans-[$PtCl_2(NH_3)$(thiazole)]

Trans-[$PtCl_2(NH_3)$(thiazole)] (PT-Tz) represents a case where the global minima of both reactants do not correspond to the proper reaction coordinates. Therefore, additional structures (labeled as R1r and R2r) have to be found in order to correctly describe the kinetic properties. In the first step, the water molecule must be located between the amine and chloride groups, closer to the sulfur atom of the thiazole ring. Nevertheless, the difference between the two total energies is very small (0.4 kcal mol^{-1}). Therefore, it can be assumed that both chloro ligands can be replaced almost equally in the first reaction step (according to the Boltzman distribution law, the ratio of local/global minima is slightly lower than 6/10). In the second step, the water molecule is located close to the hydroxy-group in the global minimum, forming a relatively strong H-bond with it. The relevant minimum for the aquation reaction was found to have the water located in the opposite quadrant, close to the remaining chloro ligand. In this case, the difference between the reaction and global minimum is much larger (about 3.4 kcal mol^{-1}). Such an energy difference would cause overestimation of the rate constant by two orders of magnitude (see below). All the structures involved on the PES of the aquation process are displayed in Fig. 2, and the lengths of the coordination bonds are summarized in Table 4. The activation barriers are about 28 and 29 kcal mol^{-1} for the first and second aquation steps, respectively. The process is also substantially less endothermic than for the Pt(dien) complex.

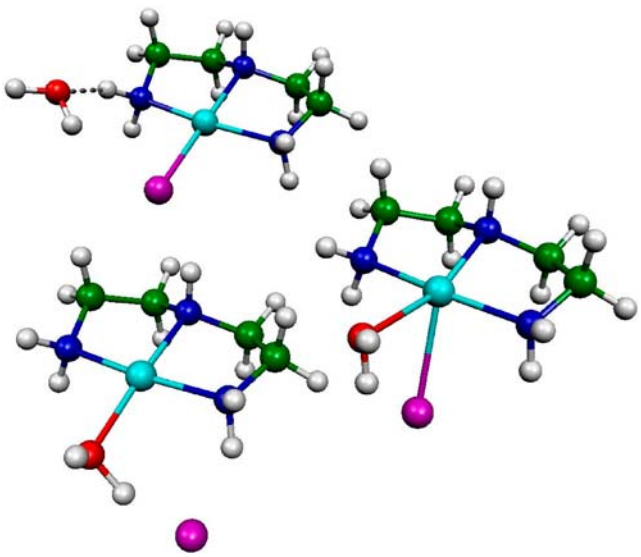

Fig. 1 Structures of stationary points on reaction coordinate of [PtCl(dien)]$^+$ [chlorodiethylenetriamine-platinum(II)]: reactant (*top left*), transition state (*right*) and product (*bottom left*)

Cis-[$PtCl_2(NH_3)$(piperidine)]

The cis-[$PtCl_2(NH_3)$(piperidine)] (Pt-Pip) complex has global minimum structure with water localized between the ammine and chloro ligand (see Fig. 3a). The geometry, with water placed between the two nitrogen atoms (which equals the global minimum in the case of cisplatin), possesses a higher energy, probably due to the hydrophobic character of the piperidine ring. There are five important stationary point structures in the second aquation step (Fig. 3b). Besides the two global minima, both additional reaction minima (at the reactant and product site) were taken into account. All three cis-Pt complexes were found to exhibit a very similar reaction profile (see Table 5). The first step is less endothermic (ca. 7 kcal mol^{-1}), with a Gibbs free energy value of about 8–9 kcal mol^{-1} and an activation barrier of about 26±1 kcal mol^{-1}. In the second step, less unique reaction barriers occur. In the Pt-Pip complex, a lower activation barrier can be found by comparing the first step and the two remaining cis-Pt complexes. This is due to the substantially less stable local (reaction) minimum, with an energy difference of about 8 kcal mol^{-1}. Thus, according to the equilibrium Boltzmann distribution, the smaller activation barrier (and higher rate constant, see below) can be compensated for by a relatively small amount (concentration) of the required reactant conformer. Similar reaction energies and Gibbs energies

Table 4 Coordination distances in the supermolecular structures of reactants (R), transition states (TS), and products (P) in the first (1) and second (2) aquation step; *r* minimum from the reaction coordinate

Complex	state	Pt-Cl_1	Pt-Cl_2	Pt-$N_{NH3/cisI}$	Pt-$N_{X/cisII}$	Pt-N_{trans}	Pt-O_1	Pt-O_2
Pt-Dien	R	2.326	-	2.066	2.081	2.065	3.690	-
	TS	2.711	-	2.064	2.070	2.050	2.340	-
	P	3.573	-	2.091	2.062	2.032	2.069	-
Pt-Tz	R1M	2.353	2.378	2.061	2.052	-	3.910	-
	R1	2.379	2.351	2.062	2.048	-	3.848	-
	TS1	2.907	2.332	2.053	2.031	-	2.415	-
	P1	3.989	2.316	2.060	2.050	-	2.110	-
	R2	-	2.359	2.064	2.042	-	2.051	3.677
	R2M	-	2.395	2.057	2.041	-	2.017	3.883
	TS2	-	2.923	2.053	2.022	-	2.001	2.474
	P2	-	3.986	2.060	2.039	-	1.988	2.123
Pt-Pip	R1	2.355	2.336	2.103	2.101	-	3.826	-
	TS1	2.819	2.340	2.031	2.077	-	2.466	-
	P1	3.975	2.338	2.095	2.065	-	2.071	-
	R2M	-	2.342	2.099	2.110	-	2.008	3.676
	R2	-	2.359	2.085	2.129	-	1.990	3.970
	TS2	-	2.826	2.072	2.106	-	2.004	2.402
	P2	-	3.939	2.047	2.112	-	2.008	2.065
	P2M	-	3.949	2.105	2.054	-	2.077	2.004
JM118	R1	2.351	2.337	2.093	2.096	-	3.694	-
	TS1	2.766	2.338	2.066	2.077	-	2.454	-
	P1	3.922	2.336	2.091	2.059	-	2.066	-
	R2M	-	2.343	2.092	2.109		1.999	3.536
	R2	-	2.355	2.084	2.123	-	1.985	3.785
	TS2	-	2.793	2.073	2.106	-	1.995	2.391
	P2	-	3.908	2.047	2.111	-	1.998	2.064
	P2M	-	4.055	2.111	2.052	-	1.991	2.080
DDP	R1M	2.326	2.326	2.098	2.098	-	3.217	-
	R1	2.342	2.334	2.100	2.093	-	3.714	-
	TS1	2.770	2.335	2.087	2.081	-	2.421	-
	P1	3.946	2.331	2.093	2.059	-	2.056	-
	R2M	-	2.340	2.093	2.105	-	1.994	3.513
	R2	-	2.352	2.118	2.084	-	1.961	3.716
	TS2	-	2.778	2.107	2.074	-	1.986	2.392
	P2	-	4.047	2.110	2.049	-	1.989	2.058

Table 5 The aquation reaction energies (ΔE_R), enthalpies ($\Delta H_{(298)}$), Gibbs free energies ($\Delta G_{(298)}$), and activation barriers (ΔE_A) (in kcal mol^{-1}). An (opt) subscript indicates the basis set used for optimization and the SP basis set used in the SP calculations

		$\Delta E_{A(opt)}$	$\Delta E_{R(opt)}$	$\Delta E_{A(SP)}$	$\Delta E_{R(SP)}$	$\Delta H_{(298)}$	$\Delta G_{(298)}$
Pt-Dien	h1[a]	30.3	22.4	31.6	23.7	22.2	23.9
Pt-Tz	h1	26.3	13.6	27.7	15.3	14.3	15.9
	h2[b]	28.2	16.3	29.3	17.1	16.2	16.7
Pt-Pip	h1	25.4	6.3	26.7	8.0	7.4	8.9
	h2	20.7	14.1	22.4	15.1	14.4	15.5
JM118	h1	22.6	3.2	25.9	8.1	7.4	8.6
	h2	23.5	10.7	28.0	14.9	14.1	14.2
DDP	h1	23.9	3.5	27.1	7.8	7.2	8.1
	h2	22.8	11.1	26.7	14.4	13.5	13.7

[a] h1 = first aquation step
[b] h2 = second aquation step

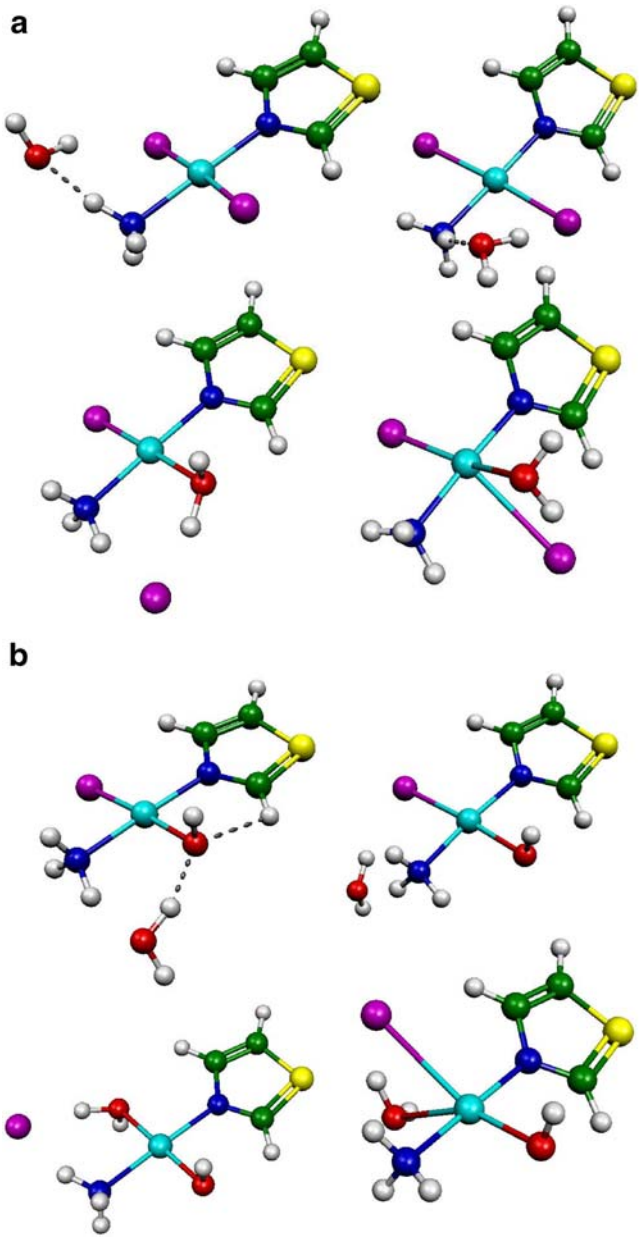

Fig. 2 Reactant, TS , and product supermolecules for the aquation reaction of the trans-[$PtCl_2(NH_3)$(thiazole)] (Pt-Tz) complex. **a** First reaction step, **b** second reaction step

were obtained for all three complexes, i.e., about 14.5± 1 kcal mol^{-1}.

Cis-[$PtCl_2(NH_3)$(cyclohexylamine)]

Cis-[$PtCl_2(NH_3)$(cyclohexylamine)] (JM118) is a metabolite and final active form of satraplatin (JM216). The geometry of the stationary points from the reaction coordinates are shown in Fig. 4. Compared with the other Pt complexes, JM118 displays the lowest activation barrier in the first aquation step, and this process is also the least energy demanding. In contrast to the Pt-Pip complex, the second reaction step can start with the global minimum structure. In this step, two transition state structures were determined. The TS21 structure (discussed below and presented in the Tables) is slightly less stable. However, it is connected with a lower activation barrier. The TS22 structure (Fig. 4b) is about 2 kcal mol^{-1} more stable than TS21, and is associated with a reaction coordinate that starts directly from the global minimum structure. This reaction coordinate has a higher activation barrier of about 2 kcal mol^{-1}. Taking into account the distribution of various reactant conformations, the reaction in gas phase will probably pass through the more demanding reaction path since the local (less stable) reaction minimum lies about 5 kcal mol^{-1} higher on the PES. Consequently, according to the Boltzmann equilibrium distribution law, this would lead to a very low population of this conformation. However, if a sufficiently large number of water molecules surrounds the Pt-complex (an assumption also necessary for the pseudo first-order reaction), it can be expected that a water molecule will be present at the required position and thus the reaction minimum (R1r) will exist. Moreover, the solvent effect will cause a further decrease in the energy difference between the global and local minima since the H-bond energy, which stabilizes the global minimum, will be reduced.

Cisplatin

Cisplatin (Cis-DDP) has a B3LYP energy profile close to the CCSD(T) results published previously [59] (although less close to MP2 values). However, use of the B3LYP method yields a different order of supermolecular conformers in the reactant state. According to MP2/6-31G(d) calculations, a water molecule is placed symmetrically between the ammine ligands in the global minimum, with the non-symmetrical reactant minimum (with water between the ammine and chloro ligands) about 0.4 kcal mol^{-1} higher on the PES. The same order was also confirmed at the CCSD(T) level, both in gas phase and in COSMO regime, and at B3LYP(COSMO)/6-31+G(d) level with an even larger energy difference of up to 1.9 kcal mol^{-1} [60]. Nevertheless, the B3LYP(gas phase) results favor the non-symmetrical arrangement by 0.9 kcal mol^{-1}.

The TS structures in all the reactions are always closer to the aquated complexes than to the chloro complexes. This is in agreement with the Hammond principle, according to which the TS structure more closely resembles the product arrangement in the endothermic reaction. This can be demonstrated by, e.g., more pronounced elongation of d(Pt-Cl) passing from reactant to TS and shortening of d(Pt-O) going from TS to product.

Rate constant estimation

Since the optimized structures, frequencies and energy profiles were obtained, the reaction rates can be estimated

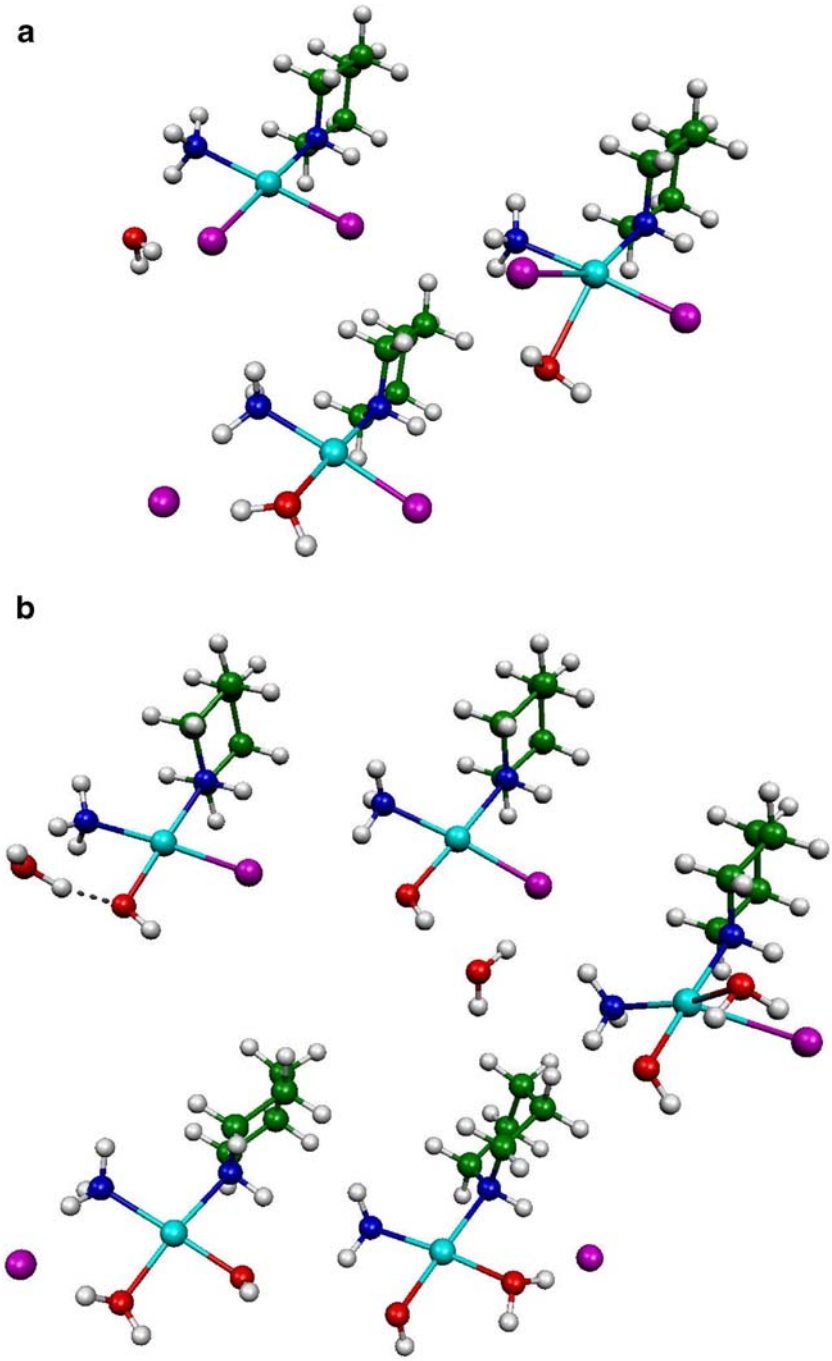

Fig. 3 Molecular structures of stationary points in the aquation reaction profile of the cis-$[PtCl_2(NH_3)(piperidine)]$ (Pt-Pip) complex. **a** First reaction step, **b** second reaction step

from Eyring TST. The determined rate constants at 298 K and 310 K are listed in Table 6. These values basically reflect the height of the activation barrier. The forward reaction can be considered as a pseudo-first-order process since the changes in the concentration of water can be neglected. Nevertheless, a backward process is the second-order reaction, it means dependent on the concentration of metallocomplex and chloride anions, which is very low in the cellular nucleus. The model used is associated with lower values of the rate constants in the second aquation step since the less stable monoaqua complex is replaced by the substantially more stable hydroxo-complex. This makes subsequent aquation more demanding. Nevertheless, this change of ligands should not play any important role in the mutual comparison of the complexes. Since the "drug" activity can, e.g., be proportional to the rate of its activation process, the Pt-Pip complex can exhibit properties very similar to those of cisplatin, while the Pt-Tz and JM118 compounds slightly differ.

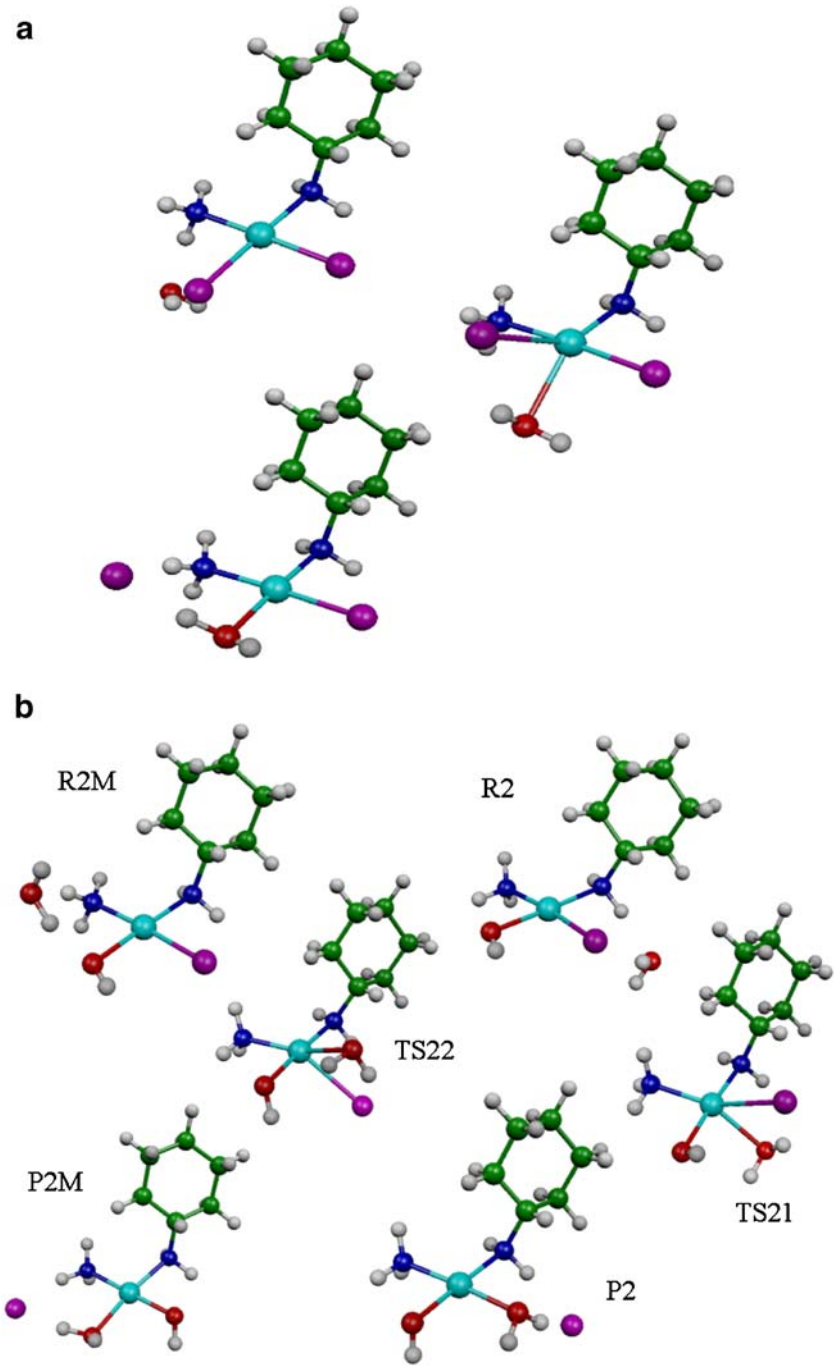

Fig. 4 Replacement reactions of chloro ligands by water molecules for the JM118 complex. **a** Exchange of the first chloride. **b** Replacement of the second chloride anion. TS22 represents the higher activation barrier for the reaction path directly from reactant global minimum structure

Bonding energies of the exchanged ligands

The association energies (bonding energies) of exchanging ligands were evaluated for the stationary point on the reaction coordinates and are presented in Table 7. It is generally accepted that the ligand replacement reactions for Pt(II) complexes pass through the associative mechanism. However, the results show that there is always only a very small energy difference between the associated water and chloride (in the reactant and product state, respectively) and between the corresponding bonding energies of these ligands in the TS. In the case of the chloro ligand, the bonding energy in the TS structure is always lower than the association energy of the remote (H-bonded) anion. The same conclusion can also be made for the water bonding energies. This means that the aquation process passes

Table 6 Rate constants for the aquation process at 298 K and 310 K

		$k_{(298)}$	$k_{(310)}$
Pt-Dien	h1	5.28E–12	4.70E–11
Pt-Tz	h1	1.20E-08	7.91E-08
	h2	2.44E-09	1.71E-08
Pt-Pip	h1	8.41E-08	5.14E-07
	h2	4.43E-06	2.32E-05
JM118	h1	3.80E-08	2.19E-08
	h2	5.68E-09	3.85E-08
DDP	h1	4.58E-08	2.86E-07
	h2	3.45E-08	2.18E-07

Table 7 Association/binding energies of replacing chloride and water/aqua ligand (in kcal mol^{-1})

		H_2O	Cl
Pt-Dien	R	−12.5	−241.7
	TS	−13.8	−190.0
	P	−56.7	−197.9
Pt-Tz	R1M	−9.4	−158.3
	R1	−9.0	−158.0
	TS1	−9.2	−118.3
	P1	−51.0	−127.6
	R2M	−14.7	−153.2
	R2	−10.2	−151.8
	TS2	−9.5	−111.8
	P2	−49.4	−121.5
Pt-Pip	R1	−10.9	−151.8
	TS1	−8.9	−112.9
	P1	−52.2	−122.1
	R2M	−16.1	−154.8
	R2	−6.0	−155.3
	TS2	−10.2	−111.5
	P2	−51.5	−118.5
	P2M	−49.3	−118.4
JM118	R1	−6.6	−154.4
	TS1	−7.8	−116.1
	P1	−53.7	−122.6
	R2M	−15.1	−154.9
	R2	−9.4	−157.3
	TS2	−7.6	−108.8
	P2	−52.2	−117.9
	P2M	−51.9	−119.1
DDP	R1M	−9.1	−158.5
	R1	−10.5	−163.4
	TS1	−8.4	−118.9
	P1	−55.7	−117.4
	R2M	−14.7	−161.0
	R2	−9.8	−162.5
	TS2	−8.9	−115.4
	P2	−54.4	−123.4

through the dissociative mechanism, or so-called facilitated dissociative mechanism (see Cooper and Ziegler [66], and Chval et al. [80]).

Comparison of aquation rate constants and cytotoxic activity

There are many reports documenting the activity of platinum drugs used in antitumor treatment [81]. Our comparison is restricted to four kinds of cancer cells: ovarian cell lines A2780, 41 M, and CH1, and the breast tumor cell line MCF-7. Table 8 compiles some experimental results of activity indexes. Some correlation between experimentally determined cytotoxic activity and calculated reaction barrier of the aquation process can be detected. Nevertheless, this simple relationship should not be overinterpreted.

Conclusions

This paper compares the electronic properties of several platinum complexes. The thermodynamic and kinetic parameters of the aquation process are also determined.

The complexes were optimized at the B3LYP/6-31++G(d,p) computational level. The analyses and reaction energy profiles were determined at the B3LYP/6-311++G(2df,2pd) level of theory. Very similar dipole moments and partial charges on the Pt atom were obtained for all three cis-Pt(II) complexes. Analogously, similar stabilization energies were found for these complexes.

The aquation process represents an activation of the platinum complexes, forming thermodynamically less stable systems. This reaction occurs due to a low chloride concentration. Aquation (as well as subsequent interactions with DNA bases) barely occurs in the Pt-dien complex due to the relatively high barrier, which makes the reaction kinetically too slow. Also, the Gibbs free energy is fairly high (24 kcal mol^{-1}). The reaction rate for remaining Pt(II) complexes can be ordered thus: Pt-Tz < JM 118 < DDP < Pt-Pip, for the first and second reaction steps. This trend partially correlates with the IC_{50} activity index of these complexes against ovarian and breast cancer cells. In some

Table 8 IC_{50} mean values (in μM)

	Pt-Dien	Pt-Tz	Pt-Pip	JM118	cDDP
A2780	>200	1.5±0.3[b]	26±3		2.2±0.6
41M	>200		64±5		26±2
CH1	>200		36±4		6±1
MCF-7		2.7±0.5[b]		1.2±0.3[a]	28.7±3.6[a]

[a] Results taken from [4]
[b] Results taken from [2], (remaining results taken from [82])

ranges, a slower rate of aquation can be correlated with a lower IC_{50} value. Therefore the antitumor activity of Pt-Pip should be greater than or comparable to cisplatin, and possibly the lowest activity (of these four complexes) can be expected in the case of Pt-TZ. However, different kinds of cancer also have different IC indexes. Therefore, this conclusion cannot be taken as generally applicable, since one simple reaction cannot be used as an estimation of a process as complex as anticancer activity without considering the additional contribution of other factors.

Acknowledgments This study was supported by grant MSM 0021620835. The computational resources from our department supercomputer cluster administrated by Dr. Šimánek should be acknowledged for providing access to excellent computational facilities.

References

1. Rosenberg B, Van Camp L, Trosko JL, Mansour VH (1969) Nature 222:385–391
2. Farrell N, Povirk LF, Dange Y, DeMasters G, Gupta MS, Kohlhagen G, Khan QA, Pommier Y, Gewirtz DA (2004) Biochem Pharmacol 68:857–866
3. Beljanski V, Villanueva JM, Doetsch PW, Natile G, Marzilli LG (2005) J Am Chem Soc 127:15833–15842
4. Wosikowski K, Lamphere L, Unteregger G, Jung V, Kaplan F, Xu JP, Rattel B, Caligiuri M (2007) Cancer Chemother Pharmacol 60:589–600
5. Najajreh Y, Kasparkova J, Marini V, Gibson D, Brabec V (2005) J Biol Inorg Chem 10:722–731
6. Marini V, Christofis P, Novakova O, Kasparkova J, Farrell N, Brabec V (2005) Nucleic Acids Res 33:5819–5828
7. Giannikopoulos G, Teo C-L, Hall MD, Fenton RR, Hambley TW (2003) Aust J Chem 56:685–689
8. Bhattacharyya D, Marzilli PA, Marzilli LG (2005) Inorg Chem 44:7644–7651
9. Malina J, Voitiskova M, Brabec V, Diakos CI, Hambley TW (2005) Biochem Biophys Res Commun 332:1034–1041
10. Brabec V, Kasparkova J (2005) Drug Resist Updat 8:131–146
11. Bivian-Castro EY, Roitzsch M, Gupta D, Lippert B (2005) Inorg Chim Acta 358:2395–2402
12. Carlone M, Marzilli LG, Natile G (2005) Eur J Inorg Chem 1264–1273
13. Barnes KR, Lippard SJ (2004) Cisplatin and related anticancer drugs: recent advances and insights. In: Sigel A, Sigel H, Sigel R (eds) Metal ions in biological systems, vol 42: Metal complexes in tumor diagnosis and as anticancer agents. Routledge, New York, pp 143–177
14. Huq F, Yu JQ, Daghriri H, Beale P (2004) J Inorg Biochem 98:1261–1270
15. Kaim W, Schwederski B (1994) Bioinorganic chemistry: inorganic elements in the chemistry of life. Wiley, Chichester
16. Takahara PM, Rosenzweig AC, Frederick CA, Lippard SJ (1995) Nature 377:649–655
17. Takahara PM, Frederick CA, Lippard SJ (1996) J Am Chem Soc 118:12309–12321
18. Yang D, van Boom SSGE, Reedijk J, van Boom JH, Wang AH-J (1995) Biochemistry 34:12912–12921
19. Gelasco A, Lippard SJ (1998) Biochemistry 37:9230–9238
20. Dunham SU, Dunham SU, Turner CJ, Lippard SJ (1998) J Am Chem Soc 120:5395–5403
21. Wing RM, Pjura P, Drew HR, Dickerson RE (1984) EMBO J 3:1201–1212
22. Lilley DMJ (1996) J Biol Inorg Chem 1:189–191
23. Coste F, Malinge JM, Serre L, Shepard W, Roth M, Leng M, Zelwer C (1999) Nucleic Acids Res 27:1837–1845
24. Spingler B, Whittington DA, Lippard SJ (2001) Inorg Chem 40:5596–5602
25. Silverman AP, Bu W, Cohen SM, Lippard SJ (2002) J Biol Chem 277:49743–49754
26. Parkinson GN, Arvanitis GM, Lessinger L, Ginell SL, Jones R, Gaffney B, Berman HM (1995) Biochemistry 34:15487–15495
27. Ohndorf U-M, Rould MA, He Q, Pabo CO, Lippard SJ (1999) Nature 399:708–712
28. Jamieson ER, Lippard SJ (1999) Chem Rev 99:2467–2498
29. Sigel H, Song B, Oswald G, Lippert B (1998) Chem Eur J 4:1053–1060
30. Williams KM, Scarcia T, Natile G, Marzilli LG (2001) Inorg Chem 40:445–454
31. Pantojaa E, Gallipolia A, van Zutphena S, Tookeb DM, Spekb AL, Navarro-Ranningerc C, Reedijk J (2006) Inorg Chim Acta 359:4335–4342
32. Kašparková J, Mackay FS, Brabec V, Sadler PJ (2003) J Biol Inorg Chem 8:741–745
33. Choi S, Delaney S, Orbai L, Padgett EJ, Hakemian AS (2001) Inorg Chem 40:5481–5482
34. Junicke H, Bruhn C, Kluge R, Serianni AS, Steinborn D (1999) J Am Chem Soc 121:6232–6241
35. Song R, Kim KM, Lee SS, Sohn YS (2000) Inorg Chem 39:3567–3571
36. Watanabe M, Kai M, Asanuma S, Yoshikane M, Horiuchi A, Ogasawara A, Watanabe T, Mikami T, Matsumoto T (2001) Inorg Chem 40:1496–1500
37. Kelland LR, Jones MM, Abel G, Harrap KR (1992) Cancer Chemother Pharmacol 30:43–50
38. Choi S, Cooley RB, Voutchkova A, Leung CH, Vastag L, Knowles DE (2005) J Am Chem Soc 127:1773–1781
39. Dal Peraro M, Ruggerone P, Raugei S, Gervasi FL, Carloni P (2007) Curr Opin Struct Biol 17:149–156
40. Baik M-H, Friesner RA, Lippard SJ (2002) J Am Chem Soc 124:4495–4503
41. Baik MH, Friesner RA, Lippard SJ (2003) J Am Chem Soc 125:14082–14092
42. Raber J, Zhu C, Eriksson LA (2005) J Phys Chem 109:11006–11015
43. Chval Z, Šíp M (2003) Coll Czech Chem Commun 68:1105–1118
44. Dos Santos HF, Marcial BL, De Miranda CF, Costa LAS, De Almeida WB (2006) J Inorg Biochem 100:1594–1605
45. Lopes JF, Menezes VSD, Duarte HA, Rocha WR, De Almeida WB, Dos Santos HF (2006) J Phys Chem B 110:12047–12054
46. Costa LA, Hambley TW, Rocha WR, Almeida WB, Dos Santos HF (2006) Int J Quantum Chem 106:2129–2144
47. Burda JV, Leszczynski J (2003) Inorg Chem 42:7162–7172
48. Burda JV, Šponer J, Hrabáková J, Zeizinger M, Leszczynski J (2003) J Phys Chem B 107:5349–5356
49. Zeizinger M, Burda JV, Leszczynski J (2004) Phys Chem Chem Phys 6:3585–3590
50. Pavelka M, Burda JV (2007) J Mol Model 13:367–379
51. Chang GR, Zhou LX, Chen D (2006) Chin J Struct Chem 25:533–542
52. Matsui T, Shigeta Y, Hirao K (2006) Chem Phys Lett 423:331–334
53. Robertazzi A, Platts JA (2006) Chem Eur J 12:5747–5756
54. Wysokinski R, Hernik K, Szostak R, Michalska D (2007) Chem Phys 333:37–48

55. Yuan QH, Zhou LX (2007) Chin J Struct Chem 26:962–972
56. Deubel DV (2002) J Am Chem Soc 124:5834–5842
57. Burda JV, Zeizinger M, Šponer J, Leszczynski J (2000) J Chem Phys 113:2224–2232
58. Zeizinger M, Burda JV, Šponer J, Kapsa V, Leszczynski J (2001) J Phys Chem A 105:8086–8092
59. Burda JV, Zeizinger M, Leszczynski J (2004) J Chem Phys 120:1253–1262
60. Burda JV, Zeizinger M, Leszczynski J (2005) J Comput Chem 29:907–914
61. Zimmermann T, Zeizinger M, Burda JV (2005) J Inorg Biochem 99:2184–2196
62. Erturk H, Hofmann A, Puchta R, van Eldik R (2007) Dalton Trans 2007:2295–2301
63. Hao L, Zhang Y, Tan HW, Chen GJ (2007) Chem J Chin Univ Chin 28:1160–1164
64. Pavelka M, Lucas MFA, Russo N (2007) Chem Eur J 13 (36):10108–10116
65. Hofmann A, Jaganyi D, Munro OQ, Liehr G, van Eldik R (2003) Inorg Chem 42:1688–1700
66. Cooper J, Ziegler T (2002) Inorg Chem 41:6614–6622
67. Zhu HJ, Ziegler T (2006) J Organometallic Chem 691:4486–4497
68. Tsipis AC, Sigalas MP (2002) J Mol Struct (Theochem) 584:235–248
69. Zhu C, Raber J, Eriksson LA (2005) J Phys Chem B 109:12195–12205
70. Song T, Hu P (2006) J Chem Phys 125:091101
71. Jia M, Qu W, Yang Z, Chen G (2005) Int J Modern Phys B 19:2939–2949
72. Robertazzi A, Platts JA (2004) J Comput Chem 25:1060–1067
73. Robertazzi A, Platts JA (2005) Inorg Chem 44:267–274
74. Zhang Y, Guo Z, You X-Z (2001) J Am Chem Soc 123:9378–9387
75. Lau JKC, Deubel DV (2006) J Chem Theor Comput 2:103–106
76. Andrae D, Haussermann U, Dolg M, Stoll H, Preuss H (1990) Theor Chim Acta 77:123–141
77. Bergner A, Dolg M, Kuechle W, Stoll H, Preuss H (1993) Mol Phys 80:1431
78. Smedarchina Z, Fernández-Ramos A, Siebrand W (2001) J Comput Chem 22:787–801
79. Weinhold F (2001) NBO 5.0 Program, University of Wisconsin, Madison, WI
80. Chval Z, Šíp M, Burda JV (2008) J Comp Chem (in press)
81. Sharp SY, Rogers PM, Kelland LR (1995) Clinical Cancer Res 1:981–989
82. Kasparkova J, Marini V, Najajreh Y, Gibson D, Brabec V (2003) Biochemistry 42:6321–6332